*metals*

MDPI

*Article*

# Corrosion Study of Implanted TiN Electrodes Using Excessive Electrical Stimulation in Minipigs

**Suzan Meijs [1,*], Kristian Rechendorff [2], Søren Sørensen [2] and Nico J.M. Rijkhoff [1]**

[1] Department of Health, Science and Technology, Center for Sensory-Motor Interaction (SMI), Aalborg University, 9220 Aalborg, Denmark; nr@hst.aau.dk

[2] Materials Department, Danish Technological Institute, 8000 Århus, Denmark; krr@teknologisk.dk (K.R.); soren.steenfeldt.moller-sorensen@LEGO.com (S.S.)

* Correspondence: smeijs@hst.aau.dk

Received: 27 February 2019; Accepted: 25 March 2019; Published: 28 March 2019


**Abstract:** (1) Background: Titanium nitride (TiN) electrodes have been used for implantable stimulation and sensing electrodes for decades. Nevertheless, there still is a discrepancy between the in vitro and in vivo determined safe charge injection limits. This study investigated the consequences of pulsing implanted electrodes beyond the in vivo safe charge injection limits. (2) Methods: The electrodes were implanted for a month and then pulsed at 20 mA and 50 mA and 200 Hz and 400 Hz. Afterwards, the electrodes were investigated using electrochemical and analytical methods to evaluate whether electrode degradation had occurred. (3) Results: Electrochemical tests showed that electrodes that pulsed at 20 mA and 200 Hz (lowest electrical dose) had a significantly lower charge injection capacity and higher impedance than the other used and unused electrodes. (4) Conclusions: The electrodes pulsed at the lowest electrical dose, for which no tissue damage was found, appeared to have degraded. Electrodes pulsed at higher electrical doses for which tissue damage did occur, on the other hand, show no significant degradation in electrochemical tests compared to unused implanted and not implanted electrodes. It is thus clear that the tissue surrounding the electrode has an influence on the charge injection properties of the electrodes and vice versa.

**Keywords:** implanted electrodes; electrical stimulation; corrosion

## 1. Introduction

Titanium nitride (TiN) has been used for implantable electrodes for many decades, starting with cardiac pacing electrodes [1]. The demands on cardiac pacing electrodes increased when it was desired to sense the heart rhythm, in order to provide rate-adaptive pacing [2]. Despite the high voltages applied during cardiac pacing, the electrode polarization should remain low so that the heart signal can reliably be recorded [1,3]. Porous electrodes were highly desirable for that purpose [4] but the electrodes should also be biocompatible [1] and corrosion resistant [3].

At the end of the previous century, TiN also received interest as a material for neural stimulation and recording electrodes [5]. Neural stimulation and recording applications within this field include, among others, visual prosthesis [6], brain implants [7,8] and cochlear implants [9]. Initially, studies reported conflicting results [5,6,9], which was likely due to differences in the fabrication method [4]. The majority of studies, however, reported very favourable properties of porous TiN [5,6], which were due to its large surface area rather than specific material properties [4].

The performance of stimulation and recording electrodes can be evaluated using their safe charge injection limits ($Q_{inj}$), charge storage capacity (CSC) and impedance. $Q_{inj}$ is evaluated by comparing the electrode polarization under pulsing conditions to the safe potential limits established using slow

sweep cyclic voltammetry (CV). The safe potential window is typically defined by the potentials at which water reduction and oxidation occurs. CSC is a measure of how much charge can be stored on the surface of the electrode and is measured using CV. The amount of charge available during fast pulsing, however, is typically much less than CSC. Impedance magnitude (typically at 1 kHz) can be used as a measure for battery consumption or recording performance. The lower the impedance, the better [10].

These properties are typically investigated under in vitro conditions in inorganic saline [5,6,9–20]. However, CSC, $Q_{inj}$ and the impedance spectrum differ under acute and chronic in vivo circumstances [4,7,8,21–28]. $Q_{inj}$ and electrode polarization have been reported to be significantly lower after implantation compared to in vitro measurements [7,8,23–27]. Moreover, they have been reported to decrease during the implanted period, when electrode failure does not occur [7,23–26].

TiN has long been known as a biocompatible [29–31] and corrosion resistant material [3,32,33], even under cathodic high voltage pulsing conditions [34]. Under anodic conditions, TiN oxidation reactions may occur, which primarily lead to passivation of these reactions until higher anodic voltages are reached [32]. At very high anodic voltages, TiN will eventually be degraded [34]. However, as $Q_{inj}$ is lower when implanted compared to in vitro [7,8,21–27], unsafe voltages may be reached during pulsing. The aim of this study was therefore to investigate whether implanted TiN electrodes would degrade during pulsing when $Q_{inj}$ measured in vivo was exceeded but $Q_{inj}$ measured in saline was not.

## 2. Materials and Methods

Four Göttingen minipigs were implanted with four working electrodes (electrode pins) and four large surface area pseudo-reference disk electrodes. Minipigs were selected because the subcutaneous adipose tissue is similar to adipose tissue in humans. The number of electrodes and pseudo-reference electrodes was chosen in order not to cause excessive discomfort to the animals and thereby also to increase the homogeneity in the results. The electrodes were made from Ti6Al4V and coated with porous TiN. The animals recovered from anaesthesia and were monitored for one month before the corrosion experiments were conducted. The work was carried out according to Danish and European legislation (ethical approval license no: 2014-15-0201-00268).

### *2.1. Electrode Fabrication*

TiN coatings were deposited on electrode pins (6 $mm^2$) made of a Ti6Al4V alloy and Ti disks (1000 $mm^2$) by reactive magnetron sputtering on a CC800/9 SiNOx coating unit (CemeCon AG, Würselen, Germany). The coatings were sputtered from four Ti targets (88 × 500 $mm^2$) with 99.5% purity in a $Ar/N_2$ mixture atmosphere. The purity of the gases was 99.999% and the $Ar/N_2$-flow was 300 sccm/350 sccm. The deposition time was 21,000 s. The electrodes underwent three-fold rotation during the coating process.

The electrodes coatings were investigated after deposition using samples taken from the same batch. Scanning electron microscopy (SEM) (Nova 600, FEI Company, Hillsboro, OR, USA) images were taken at magnifications ranging from 450× to 25,000× to get an overview of the surface and to investigate the surface structure of the electrodes in detail. A silicium sample coated in the same process was used to study the thickness, homogeneity and porous structure of the TiN coating using SEM. Images were recorded at a magnification of 40,000×.

An ethylene tetrafluoroethylene (ETFE) coated 35N LT wire (Heraeus, Yverdon, Switzerland) was crimped to the hollow end of the electrode pins. A polyether ether ketone (PEEK) body and silicone tines were produced using injection moulding to insulate the electrode pins. The tines were first glued to the PEEK body using a silicone adhesive. The PEEK body with tines was then glued to the electrode pins also using a silicone adhesive. Further details and figures of the electrode production can be found in Reference [24]. The electrodes were cleaned thoroughly before they were sterilized by an overdose of electron-beam processing.

### 2.2. Surgical Procedure

For electrode implantation, the animals were anesthetized using Propofol. Small incisions were made in the back and the electrodes were implanted using a custom-made implantation tool. This ensured that the electrodes were placed in tight pockets in subcutaneous adipose tissue, which promotes fast healing and ingrowth. Five electrodes were implanted into each pig, four of which were used for intense electrical stimulation and one electrode in each pig served as a control. Four counter electrode disks with a percutaneous wire were also implanted in each pig. The minipigs recovered from the procedure and were carefully monitored in order to detect and treat cases of infection. The electrodes were not used for one month until the pigs were anaesthetized again using sevoflurane to perform electrical stimulation. After the stimulation sessions were completed, the electrodes were carefully dissected from the tissue. The electrodes were extensively cleaned using demineralized water and alcohol, they were then rinsed and stored dry, so that they could be further investigated.

### 2.3. Electrical Stimulation

Electrical stimulation was performed using a DS5 (Digitimer, Hertfordshire, UK) per electrode. The device was shorted between the pulses using a custom-build set-up to prevent drifting of the baseline potential. Biphasic, charge balanced 200 µs square pulses were applied, cathodic first with an inter-phase interval of 40 µs during which no current was applied. Stimulation was performed for 6 h in total, divided into three 2-h sessions. Before, between and after these sessions, voltage transient measurements (VTM) were recorded for each electrode using a VersaSTAT 3 potentio-galvanostat (Princeton Applied Research, Oak Ridge, TN, USA).

Four stimulation paradigms were applied:

- Group 1: 20 mA, 200 Hz
- Group 2: 20 mA, 400 Hz
- Group 3: 50 mA, 200 Hz
- Group 4: 50 mA, 400 Hz

During pilot experiments, it was verified that the group 1 stimulation paradigm did not cause tissue damage after one week of implantation (see Figure S1). To cause electrode damage, we decided to increase 2 parameters: stimulation frequency and stimulation amplitude. The stimulation frequency was doubled, which was expected to cause electrode damage due to an increasing trend in the inter-pulse potential [35]. The stimulation amplitude was set to the maximum the DS5 can deliver, which was expected to cause electrode damage by increasing the electrode potential during stimulation. It was expected that group 2–4 protocols would result in tissue damage; therefore photographs were taken of the tissue surrounding the electrodes to document the amount of tissue damage. However, the focus of this study is corrosion and the electrodes were thus investigated more extensively using electrochemical and analytical methods.

During stimulation, the voltage transients were recorded every 30 min using an oscilloscope. From these voltage transients, the resistive drop after pulse cessation (IR-drop) was calculated as [10]:

$$\text{IR-drop} = E_{\text{pulse\_end}} - E_{\text{pulse\_end+40}} \quad (1)$$

where $E_{\text{pulse\_end}}$ is the recorded potential at the end of the cathodic pulse and $E_{\text{pulse\_end+40}}$ is the potential 40 µs after pulse cessation (see Figure 1) [10]. $E_{mc}$ and $E_{ma}$ are the maximum cathodic and anodic voltage excursions after IR-drop is subtracted from the original voltage transient.

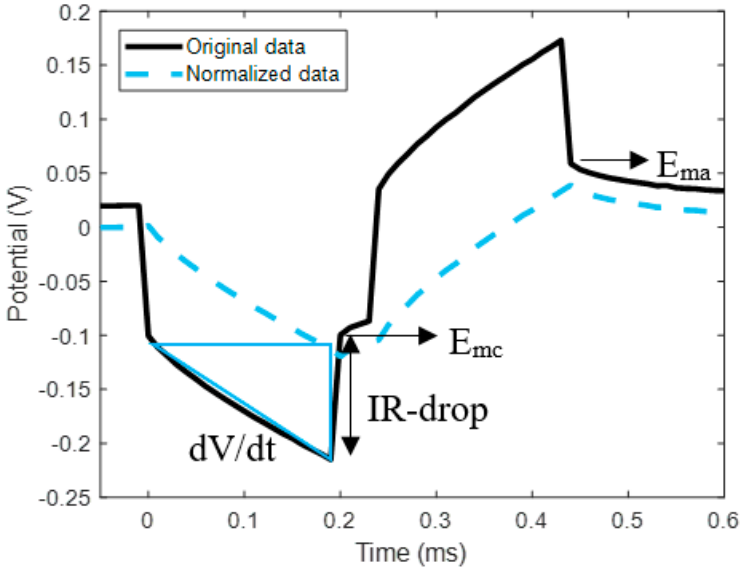


**Figure 1.** IR-drop, dV/dt, $E_{mc}$ and $E_{ma}$ are derived from the original data, while in the manuscript normalized data are presented. The data is normalized by subtracting the IR-drop and setting the pre-pulse potential to 0.

VTM before, between and after the stimulation blocks, was performed using the VersaSTAT 3 potentio-galvanostat using the same stimulation pulse.

The pulsing capacitance ($C_{pulse}$) was computed using the slope (dV/dt) of the voltage transient:

$$I_{stim} = C_{pulse} \cdot \frac{dV}{dt} \quad (2)$$

where $I_{stim}$ is the stimulation current (1 mA while implanted and 5 mA in the electrochemical characterization). $Q_{inj}$ was calculated using the current ($I_{max}$) at which $E_{mc}$ or $E_{ma}$ reached the safe potential limits (−0.6 and 0.9 V vs. open circuit potential, respectively) [10,24]:

$$Q_{inj} = \frac{I_{max} \cdot t}{A} \quad (3)$$

where t is the pulse duration (200 µs) and A is the geometrical surface area of the electrodes (6 $mm^2$). When voltage excursions exceeded machine limits (±10 V), $I_{max}$ was extrapolated from the highest current assuming a linear relation.

$$V_{ext} = V_m \left(1 + \frac{I_{ext} - I_m}{I_m}\right) \quad (4)$$

where $V_m$ and $I_m$ were the measured potential and current, respectively, and $V_{ext}$ and $I_{ext}$ were the extrapolated potential and current. When $V_{ex}$ reached the potential limits, $I_{ext}$ was used as $I_{max}$ in (3). This method provided accurate results using data for which $I_{max}$ was measured.

### *2.4. Coating Characterization*

After explantation, all electrodes were characterized using SEM and energy-dispersive x-ray spectroscopy (EDX). The electrochemical properties were investigated using electrochemical impedance spectroscopy (EIS), CV and VTM. Two electrode groups were added to the 4 groups of active implants, therefore these measurements were performed on six electrode groups:

- Group 1: implanted—20 mA, 200 Hz
- Group 2: implanted—20 mA, 400 Hz

- Group 3: implanted—50 mA, 200 Hz
- Group 4: implanted—50 mA, 400 Hz
- Group 5: implanted controls
- Group 6: not implanted controls

SEM (Nova 600, FEI Company, Hillsboro, OR, USA) images were recorded at magnifications varying from 450× to 10000× to obtain an overview of the surface and to investigate in detail the surface structure of the electrodes. SEM images of the not implanted control electrodes (group 6) were made, both to compare to the other electrode groups, as well as to investigate the uniformity of the coating after deposition. Further SEM analysis was carried out on a Si-wafer which was coated in the same process as the electrodes. The Si-wafer was mounted in a manner similar to the electrodes and the measured thickness is representative for the coating thickness on the electrodes. The advantage of using Si-wafer is that a cross-section analysis of the coating can be done easily. EDX (EDAX, AMETEK, Leicester, UK) spectra were made to investigate the chemical composition of the coatings after deposition and to determine whether the surface chemistry of the electrodes changed after having been implanted and after intense pulsing.

Electrochemical characterization measurements were performed in an electrochemical cell at room temperature using phosphate buffered saline as the electrolyte. The measurements were performed in a 3-electrode set-up, using the above mentioned porous TiN electrodes as working electrodes (0.06 $cm^2$), a Ag | AgCl reference electrode (1.6 $cm^2$) and a platinum foil counter electrode (50 $cm^2$).

Solartron, Model 1294 in conjunction with 1260 Impedance/gain-phase Analyzer (Solartron Analytical, Farnborough, UK) were used to perform EIS measurements. Accompanying SMaRT software was used to run the measurements. A sinusoidal current was used at frequencies from 0.1 Hz to 100 kHz, with 10 measurements per decade. Three different currents (5, 10 and 50 μA) were used to ensure that the measurement currents were in the linear operation range of the electrode [36]. An integration time of 10 s was used to obtain a reliable and noise-free signal.

Cyclic voltammetry (CV) was performed by cycling the electrode potential was cycled between the safe potential limits (−0.6 and 0.9 V vs. Ag | AgCl) previously established for similar electrodes [24]. The sweep rates used for CV were 0.05, 0.1, 0.5 and 1.0 V/s. Ten cycles were made at each sweep rate, the last cycle was used for data analysis. The cathodic charge storage capacity (CSC) was derived from the CV by taking the integral of the CV below the zero-current axis [10].

VTM were conducted in the same manner as described above for the implanted electrodes, except the 3-electrode setup and the electrochemical cell were employed. The maximum charge injection limit ($Q_{inj}$) and pulsing capacitance ($C_{pulse}$) were derived according to Equations (1)–(3).

### *2.5. Statistics*

The data recorded during the 2-h pulsing sessions using an oscilloscope were filtered using a low-pass Butterworth filter (passband 5 kHz, stopband 15 kHz). $E_{mc}$ and IR-drop were then normalized to the first measurement (session 1, start). $E_{mc}$ was selected for statistical analysis to represent the electrode polarization and $IR_{drop}$, as a measure of the tissue resistance. Before, between and after the pulsing sessions, voltage transients were recorded using the VersaSTAT 3 (Princeton Applied Research, Oak Ridge, TN, USA). From these voltage transients $Q_{inj}$ and $C_{pulse}$ were used to further quantify the electrochemical performance of the electrodes. A linear mixed model was used to statistically analyse the data. Parameters (group, session, time and combinations thereof) were added stepwise to the model, until adding another parameter did not make a significant difference to the model.

One-way ANOVA was used to investigate the electrochemical properties of the electrodes after explantation (electrochemical cell setup). The following electrochemical properties of the 6 different electrode groups were used for statistical analysis:

- Cathodic CSC at 0.05 and 1.0 V/s
- Impedance magnitude at 0.1 Hz

- $Q_{inj}$

Significant findings are reported at p-values smaller than 0.05.

## 3. Results

All implantations were carried out without any complications. The animals recovered well from the surgery and no infections were observed during the month the electrodes were implanted.

### *3.1. General Coating Characteristics*

In contrast to the well-known yellow-golden coloured TiN, the coatings on the electrodes had a brownish colour. To analyse the structure and chemical composition of the coating, the electrodes were studied in SEM and EDX. The overview SEM image (Figure 2a) shows a uniform coating on the electrode and in the corresponding EDX spectrum (Figure 2b) the expected peaks belonging to Ti and N are present. The quantification of the amounts of Ti and N from an EDX spectrum is difficult because the K-line of N and the L-line of Ti are very close. Here, numbers close to a 1:1 atomic ratio of Ti to N are found (note that weight-% is used in Figure 2b). The SEM images in Figure 3a clearly show a faceted structure, typical for TiN deposited at high pressure. The cross-section SEM image in Figure 3b shows the porous morphology of the coating as well. The coating thickness is approximately 6 µm.

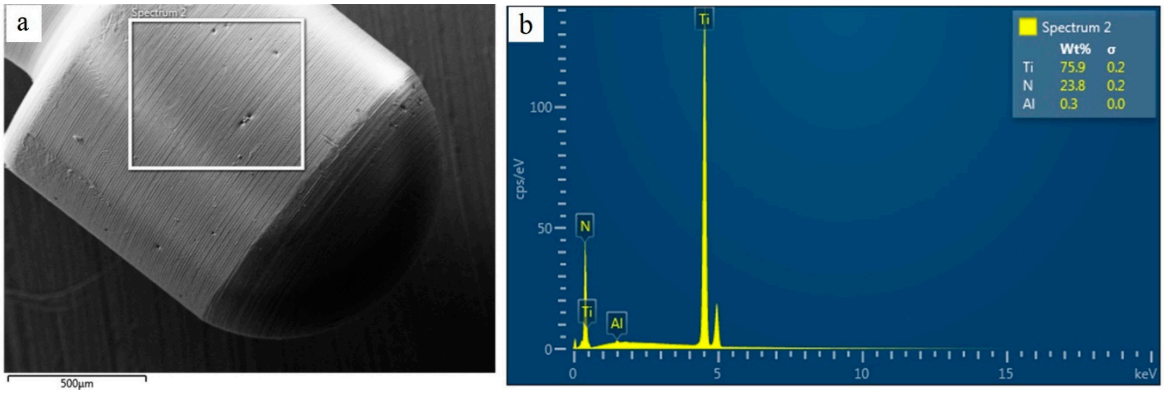


**Figure 2.** (**a**) Scanning electron microscope (SEM) image of the coated electrode. The indicated region is the area over which EDX was performed. The scale-bar is 500 µm. (**b**) Typical energy dispersive X-ray spectroscopy (EDX) spectrum corresponding to the area indicated in (**a**).

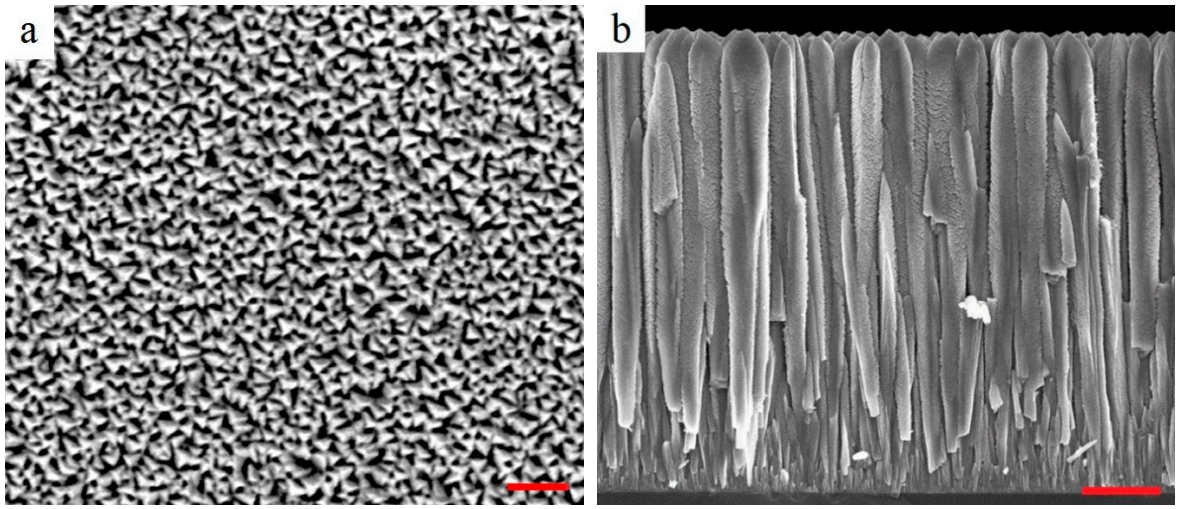


**Figure 3.** (**a**) Top-view (magnification: 25,000×) and (**b**) cross-section SEM images (magnification: 40,000×) of TiN coating on Si-wafer. Scale bar: 1 µm.

### *3.2. Changes in Electrochemical Properties during Intensive Pulsing*

The shorting part of the setup broke down during the last series of measurements. The last two stimulation sessions could therefore not be completed with one of the electrodes in the 20 mA—00 Hz group. The data obtained with this electrode after the breakdown was not used in the analyses.

The significant parameters of the statistical model for IR-drop were: Time, Session, Group × Session and Time × Session. For $E_{mc}$, Group was an additional significant parameter of the statistical model. Figure 4 shows that the results for IR-drop and $E_{mc}$ were similar. Both IR-drop and $E_{mc}$ were significantly larger during session 1 compared to sessions 2 and 3 for electrode groups 2, 3 and 4. IR-drop and $E_{mc}$ were only significantly larger during session 1 compared to sessions 2 and 3 at the 30 and 60 min measurements. Figure 4a,b also show that IR-drop (for groups 2, 3 and 4) and $E_{mc}$ (all groups) were significantly larger after 30 and 60 min of pulsing compared to after 90 and 120 min of pulsing during session 1.

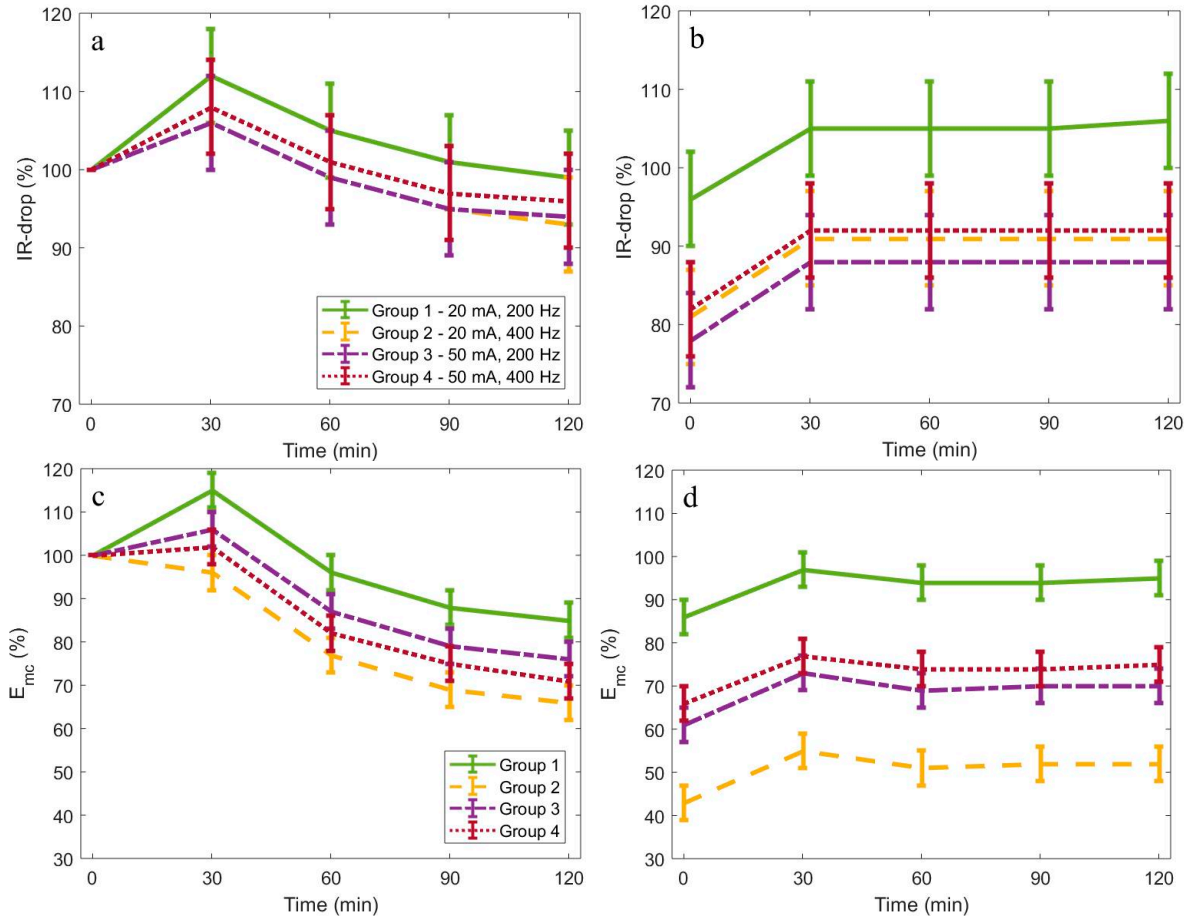


**Figure 4.** (**a**) IR-drop increased from baseline and then decreased during the first pulsing session for electrode groups 2, 3 and 4. (**b**) During session 2 and 3 (shown), an increase in IR-drop was seen from the start of stimulation, after which IR-drop remained stable. The IR-drop of group 2, 3 and 4 electrodes was significantly smaller during sessions 2 and 3 compared to session 1. (**c**) The same trend was observed for $E_{mc}$ of all electrode groups but to an even greater extent (notice the axis). (**d**) An increase in $E_{mc}$ was also observed from the start of stimulation during sessions 2 and 3 (shown). $E_{mc}$ of group 2, 3 and 4 electrodes was also significantly smaller during sessions 2 and 3 compared to session 1 but notice again the difference in the axis of IR-drop and $E_{mc}$.

$E_{mc}$ of group 1 electrodes was significantly larger than $E_{mc}$ of group 2, 3 and 4 electrodes in all sessions. During session 2, $E_{mc}$ of group 2 electrodes was significantly smaller than $E_{mc}$ of group 1 and 3 electrodes and during session 3 $E_{mc}$ of group 2 electrodes was significantly smaller than $E_{mc}$ of group

1, 3 and 4 electrodes. Figure 4c,d show that IR-drop and $E_{mc}$ of all electrode groups was significantly smaller at the start of stimulation compared to after 30, 60, 90 and 120 min of pulsing during session 3. The same was found for session 2.

### 3.3. Changes in Electrochemical Properties between Pulsing Sessions

For both $C_{pulse}$ and $Q_{inj}$, the significant fixed effects were: Time, Group and Time*Group. The results of the statistical analysis for $C_{pulse}$ and $Q_{inj}$ were identical, except for a baseline difference between electrode groups observed for $Q_{inj}$ ($p = 0.045$). $Q_{inj}$ of group 2 electrodes ($8.3 \pm 2.4$ μC/cm$^2$) was significantly smaller than $Q_{inj}$ of group 3 and 4 electrodes ($15.8 \pm 2.4$ μC/cm$^2$).

Figure 5a,b show that $Q_{inj}$ and $C_{pulse}$, respectively, of group 1 electrodes did not change significantly. For group 2, 3 and 4 electrodes, $Q_{inj}$ increased significantly to values of $26.45 \pm 2.7$ μC/cm$^2$, $50.00 \pm 2.4$ μC/cm$^2$ and $52.50 \pm 2.4$ μC/cm$^2$, respectively, after 6 h of intense pulsing. $C_{pulse}$ of electrode groups 2, 3 and 4 increased significantly to capacitances of $54.1 \pm 5.4$ μF/cm$^2$, $97.1 \pm 4.9$ μF/cm$^2$ and $106.0 \pm 4.9$ μF/cm$^2$, respectively. Figure 5c,d show that the increase in $C_{pulse}$ caused a decrease in electrode polarization. This decrease in electrode polarization led to an increased $Q_{inj}$.

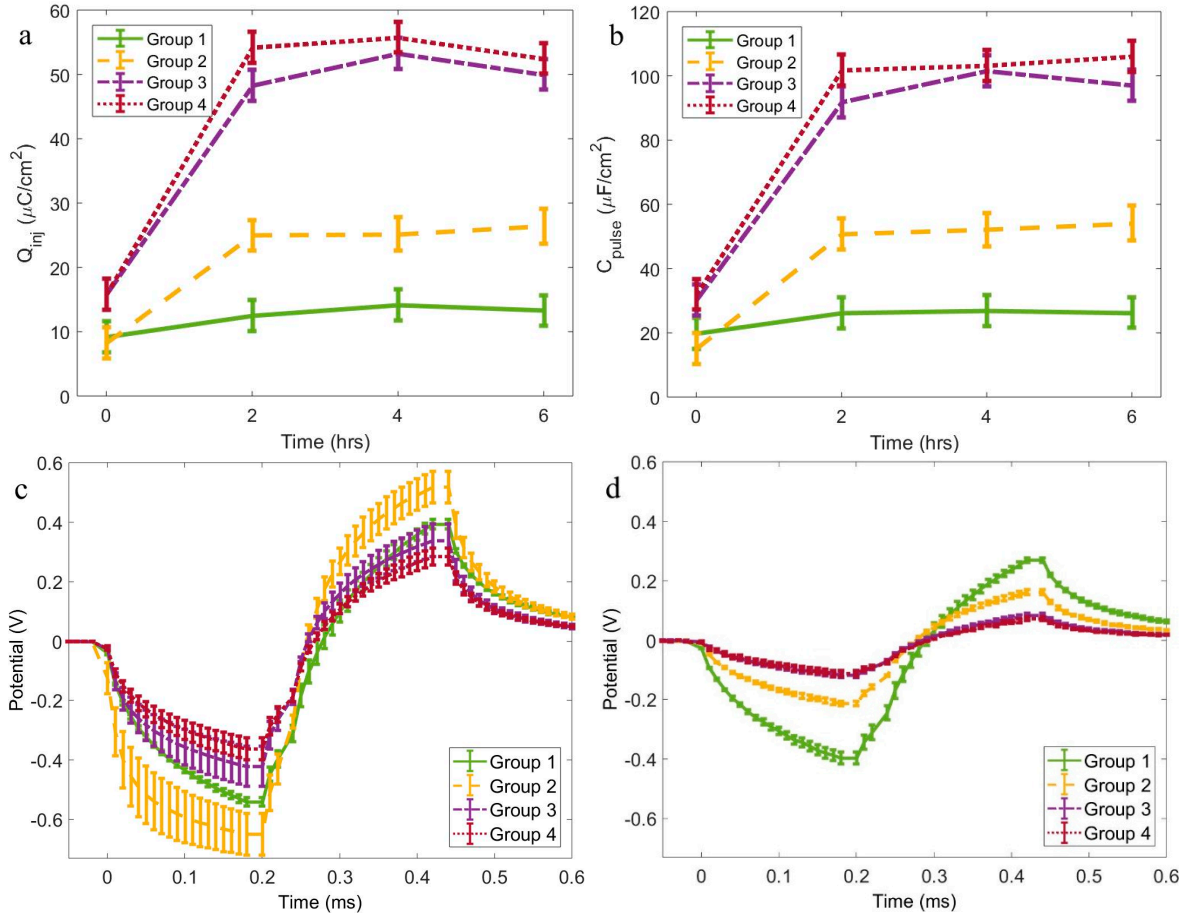


**Figure 5.** (**a**) After the first pulsing session $Q_{inj}$ was increased compared to before pulsing for electrode groups 2, 3 and 4. (**b**) The same was observed for $C_{pulse}$ of electrode groups 2, 3 and 4. (**c**) Normalized voltage transients recorded before pulsing at 3 mA. (**d**) Normalized voltage transients recorded at 3 mA after 2 h of pulsing.

Electrode group 1 had a significantly smaller $Q_{inj}$ than all other electrode groups after the first pulsing session, which remained after the second and third pulsing session. Furthermore, electrode group 2 had a significantly smaller $Q_{inj}$ than electrode groups 3 and 4 after the first pulsing session.

This difference also remained significant after pulsing sessions 2 and 3. The same group differences were observed for $C_{pulse}$.

### 3.4. Electrochemical Characteristics after Explantation

The results of the electrochemical characterization in phosphate buffered saline were largely consistent across measurements, as shown in Figure 6. Group 1 electrodes had a significantly smaller CSC at 0.05 and 1.0 V/s and a significantly larger impedance magnitude at 0.1 Hz compared to all other electrode groups. They also had a significantly smaller $Q_{inj}$ compared to group 2 electrodes and the control electrodes in groups 5 and 6. But the $Q_{inj}$ of group 1 electrodes was not significantly different from group 3 and 4 electrodes.

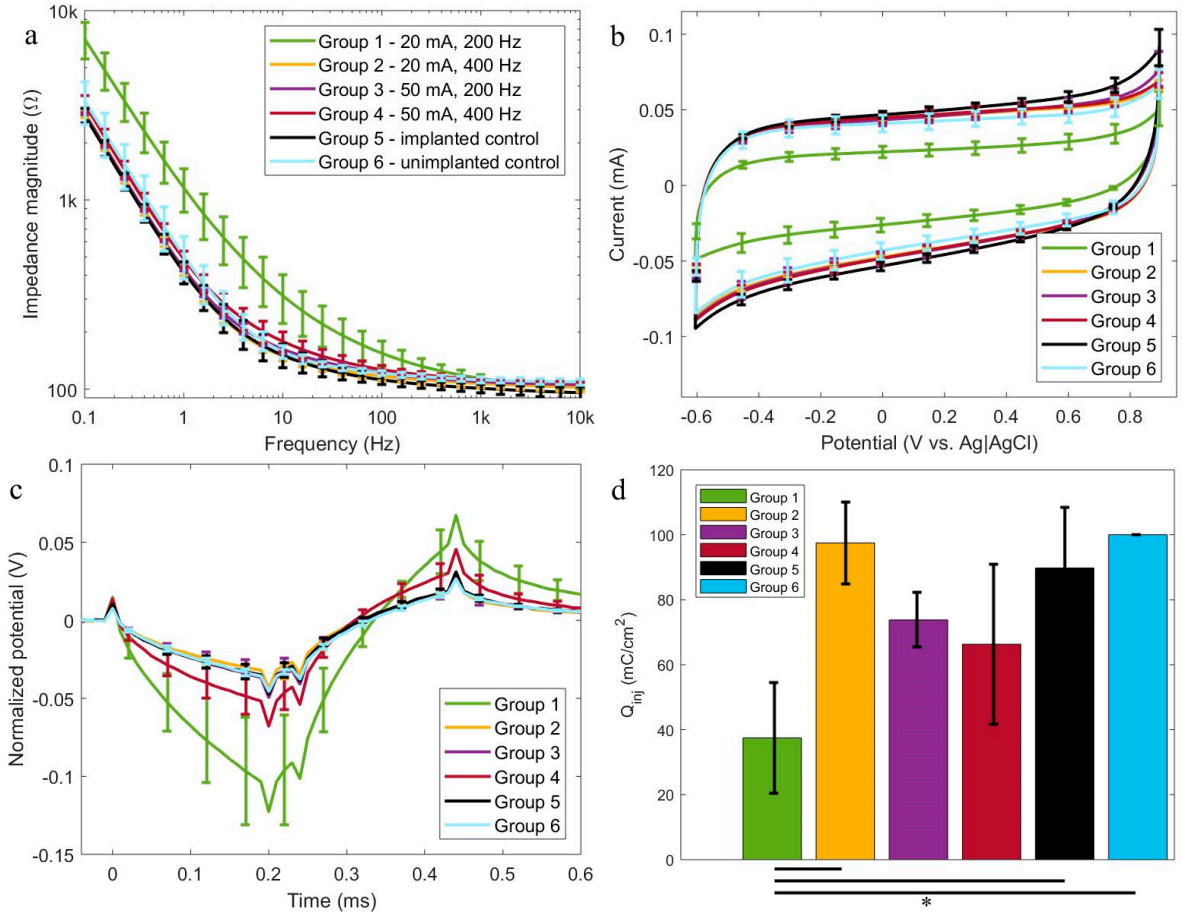


**Figure 6.** (**a**) The impedance magnitude was significantly larger for electrode group 1 compared to the other electrode groups, which was implanted and pulsed at the lowest electrical dose. (**b**) The cyclic voltammogram shows that the charge storage capacity of electrode group 1 was significantly smaller than the other electrode groups. (**c**) The normalized voltage transients at 5 mA show that the slope of the group 1 electrodes was larger than the slopes of the other electrode groups but no significant difference was found for $C_{pulse}$. (**d**) $Q_{inj}$ of group 1 electrodes was significantly smaller than $Q_{inj}$ of group 2, 5 and 6 electrodes.

### 3.5. Coating Properties after Explantation

SEM images (see Figure 7) showed that the electrode surfaces were intact after 6 h of intense stimulation. The coatings were all undamaged and had the same faceted structure, which is typical for TiN, as the electrodes had after deposition of the coating. Figure 7 indicates that there were no differences in chemical composition of group 1 and group 4 electrodes. The EDX spectra of all electrodes in all groups showed similar levels of titanium, nitrogen and oxide.

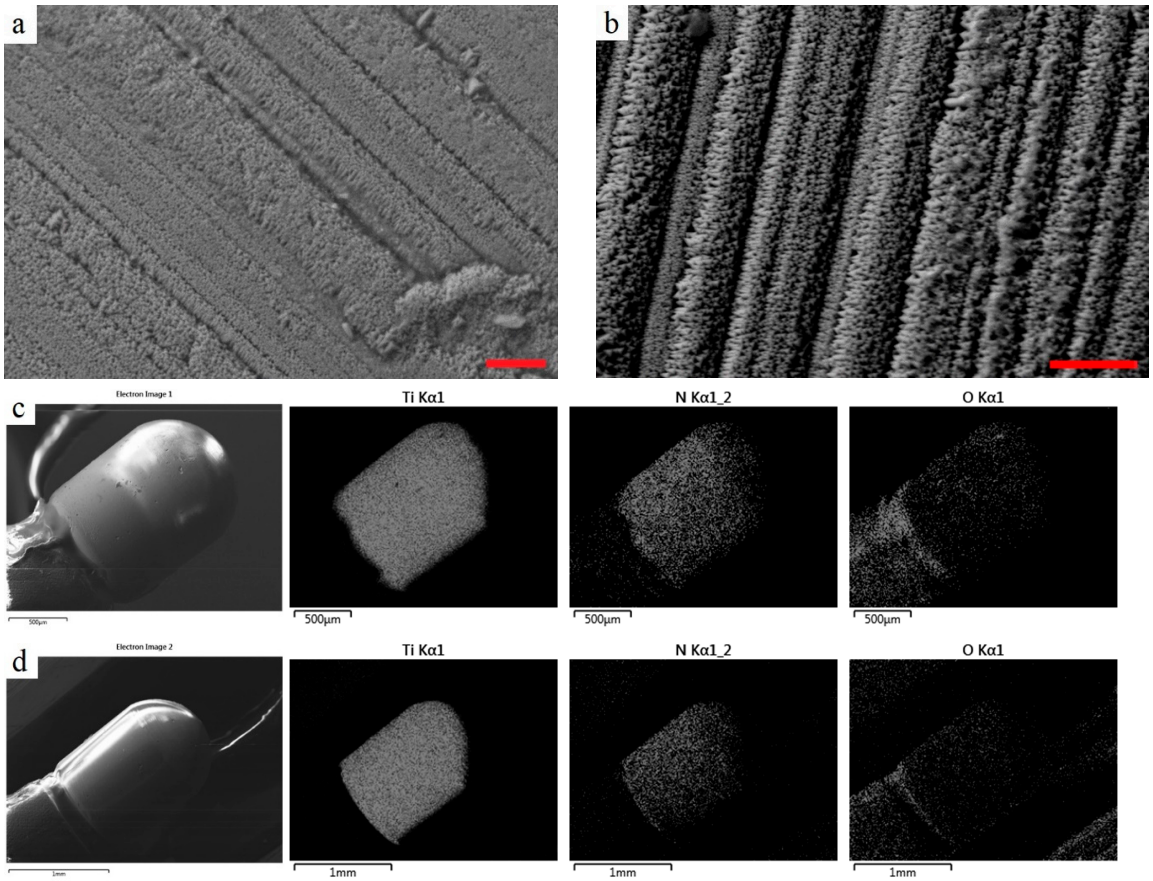


**Figure 7.** (**a**) Close-up SEM image (magnification: 10,000×) of an electrode in group 1 (20 mA—200 Hz), showing that the surface structure is still intact (scale bar: 10 µm). The same is true for (**b**), showing the detailed structure of an electrode in group 4 (50 mA—400 Hz, scale bar: 10 µm, magnification: 15,000×). (**c**) Overview SEM (magnification 450×) and corresponding EDX images of an electrode in group 1 show that the chemical composition of the electrode surface after pulsing was very similar to (**d**) the chemical composition of the electrode surface of an electrode in group 4. Also visualized by an overview SEM (magnification 450×) and corresponding EDX images of an electrode in group 4.

## 4. Discussion

Several previous studies [37–39] have shown that TiN coatings grown at high N-partial pressures become porous. These coatings have a brown colour that clearly distinguish them from the standard golden-coloured TiN used on tools and components. For use in electrode applications, it is essential to use the porous type of TiN coating as they have a high effective surface area, which in turn leads to a low impedance [3,4]. Cunha et al. [39] did a systematic study of the influence of N-content of the morphological structural and electrochemical properties of TiN coatings. In the case of high N-content (Ti:N ratio 1:1.34), these authors obtain results similar to ours regarding the coating morphology. The reason for the discrepancy in chemical composition (in our case we measure a Ti:N ratio 1:1 with EDX) could be that Cunha et al. [39] have determined the chemical composition using Rutherford Backscattering Spectrometry, which provides a more precise determination compared to EDX. Other studies have found that porous near-stoichiometric TiN coatings can be obtained just by adjusting the energy available during film growth [40].

Six groups of electrodes were used in this study, five of which were implanted and four of which were used for 6 h of intense pulsing at different electric doses:

- Group 1: 20 mA, 200 Hz
- Group 2: 20 mA, 400 Hz

- Group 3: 50 mA, 200 Hz
- Group 4: 50 mA, 400 Hz
- Group 5: implanted controls
- Group 6: un-implanted controls

During intense pulsing, IR-drop was derived from the voltage transients as a measure of tissue impedance and $E_{mc}$ was used as a measure of electrode polarization. Between the three 2-h pulsing sessions, $Q_{inj}$ was evaluated and from these voltage transients $C_{pulse}$ was derived.

No significant changes were observed during intense pulsing for group 1 electrodes, receiving the lowest electrical dose. For group 2, 3 and 4 electrodes the IR-drop and $E_{mc}$ decreased and $Q_{inj}$ and $C_{pulse}$ increased. The stability in pulsing properties of group 1 electrodes together with the fact that these electrodes received the lowest electrical dose, would intuitively lead to the expectation that these electrodes did not corrode [4,7,8,23–26]. For group 2, 3 and 4 electrodes, on the other hand, it could be expected that corrosion may have occurred, even though the observed electrochemical changes are favourable in the light of pulsing capability (higher charge injection, lower electrode polarization). Passivation at high anodic potentials was the main expected corrosive reaction [33,34], leading to decreased pulsing capability. Excessive bubbling due to water reduction [34], however, may lead to cracking of the coating. This could increase the surface area and thereby lead to an apparent increase $Q_{inj}$. The results of the electrochemical characterizations after explantation showed that group 1 electrodes had significantly deteriorated electrochemical properties compared to all other electrode groups. Group 2, 3 and 4 electrodes, on the other hand, had no different electrochemical properties after explantation than the two control groups (5 and 6).

Analytical investigations could neither confirm nor reject the electrochemical results. SEM images show that all coatings seemed to be intact. EDX spectra did not reveal differences between the harshest and mildest stimulated electrodes either. However, it must be noted that it is difficult to distinguish between the oxygen and nitrogen signal using EDX because the K-peaks of the two elements are quite close. As oxidation of the coating could have occurred, other analytical methods have been attempted (X-ray photoelectron spectroscopy and Time-of-Flight Secondary Ion Mass Spectrometry) in order to detect any differences in oxygen amounts. Preliminary results were unsuccessful, mainly because the geometry and size of the electrode is quite challenging in both the experimental set-ups. It is, however, very unlikely that the coating oxidized without showing any signs of damage. Norlin et al. [34] show SEM images porous TiN electrodes after anodic pulsing, which are severely damaged. For the current electrodes no signs of damage were found using SEM and EDX analysis.

Corrosion studies of stimulation electrodes have been performed extensively in saline [3,34,41–43]. Some studies found that the damage threshold is exactly at the water window limit [43], others suggest that the water window limit may be too conservative under pulsing conditions [41,44] and yet others suggest that corrosion may occur even within the limits of water reduction and oxidation [42]. TiN has been most extensively investigated by Norlin et al. [3,34,45]. Their pulsing study was carried out using 700V pulses of both anodic and cathodic polarity [34]. As expected, TiN showed severe corrosion upon anodic pulsing but was stable when cathodic pulses were applied. The voltages recorded in this study during constant current pulsing were, however, a factor 15–30 smaller. In a later study, the electrodes were aged using more conservative voltages (−3 and 1 V vs. Ag | AgCl), corresponding to 4 months of use based on the charge passed [3]. TiN proved very stable, which was expected, as high anodic voltages were avoided. In the current study, very high anodic voltages were also avoided by using a cathodic first stimulation paradigm. Anodic voltages between 1 and 3 V (vs. open circuit potential) were observed with the highest voltages in the 50 mA groups (groups 3 and 4). No signs of corrosion were observed for the electrodes in those groups, while corrosion of the anodically pulsed samples by Norlin et al. [34] was obvious in SEM images.

It has also been shown before that safe limits obtained in inorganic solutions do not necessarily apply to electrodes in protein containing solution [46] and implanted electrodes [47,48]. It was therefore concluded that proteins must protect the electrode surface against corrosion [46,48,49]. However,

$Q_{inj}$ was never measured in vivo for these electrodes and it is therefore unclear whether or not it was exceeded [47,48]. The in vitro water window limits for platinum were not exceeded in either of the studies but in both studies corrosion was observed nevertheless [47,48]. Shepherd et al. [48] argue, however, that corrosion was not stimulation-induced but due to production failures. In the current study, $Q_{inj}$ (measured in vivo) was exceeded for all stimulated electrode groups (1, 2, 3 and 4) during all stimulation sessions. However, group 1 and 2 electrodes were pulsed at approximately 20% of $Q_{inj}$ as measured in saline and groups 3 and 4 electrodes were pulsed at approximately 50% of the in vitro $Q_{inj}$. Robblee et al. [47] stimulated their electrodes at approximately 5% and 30% of $Q_{inj}$ in vitro. They observed platinum dissolution for all electrodes pulsed at 30% of $Q_{inj}$ (in vitro) and less for electrodes pulsed at 5%. Shepherd et al. [48] stimulated the electrodes at 5-10% of $Q_{inj}$ in vitro but concluded that the observed corrosion was not stimulation-induced. This makes it obvious that in vitro safe limits cannot be applied in vivo. However, it does not rule out that limits measured in vivo using techniques developed in vitro may be too conservative.

Interestingly, we found that corrosion most likely occurred for the electrodes pulsed at the lowest electrical dose (group 1 electrodes; 20% of $Q_{inj}$ in vitro and 200 Hz). As group 2, 3 and 4 electrodes showed no signs of corrosion in the electrochemical characterizations after explantation, the occurrence of corrosion seems not only dependent on the electrode potentials or charge delivered. We suspect that the occurrence of corrosion is not only medium dependent (organic vs. inorganic, basic vs. acidic) but also tissue dependent. Although tissue damage was not the focus of this study, it seems to play an important role. No tissue damage seems to have occurred for electrode group 1, while tissue damage with increasing severity occurred for electrode groups 2–4 (see Figure S2). The lack of tissue damage for electrode group 1 is confirmed by the lack of change in IR-drop, which is representative of tissue impedance [10]. The same amount of charge density per phase was injected for electrode groups 1 and 2 but due to the increased frequency tissue damage is likely to have occurred in group 2 [50,51]. Tissue damage obviously occurred in electrode groups 3 and 4 (see Figure S2). Based on the IR-drop data, it appears that the tissue was damaged during the first hour of the first pulsing session for electrode groups 2, 3 and 4. It seems that a new electrode-tissue interface was formed that remained during pulsing session 2 and 3. This new electrode-tissue interface allowed for more charge injection, as $Q_{inj}$ and $C_{pulse}$ were significantly increased after the first pulsing session compared to before pulsing. And although the electrodes were still pulsed beyond the increased $Q_{inj}$ in vivo, the formation of a new electrode-tissue interface and corresponding increase in $Q_{inj}$ may thus have prevented corrosion.

The electrode-tissue interface appears to play a very important role with regards to the occurrence of corrosion. These results can therefore only be applied to stimulation electrodes implanted in adipose tissue, like ours [23,24,52] and like Bion [53] for example. They cannot be applied to implants in the brain [47], the cochlea [48] or the blood stream [1,2,4]. Furthermore, our electrode is a macro-electrode (0.06 $cm^2$). There are indications that different charge injection limits apply to smaller microelectrodes [51]. These results might therefore not apply to microelectrodes. Lastly, as it is challenging to work with larger animals, such as minipigs, the number of animals is low compared to rodent studies for example. The results, however, are consistent across measurements and rather homogeneous within the electrode groups and were thus statistically significant.

With the recent increase in investment in "electroceuticals," the development of novel, smaller and more sophisticated implants may be anticipated [54]. It is therefore more important than ever before to establish safe limits that apply to these specific implants [51]. We show that this is not only relevant in the light of tissue damage but also with respect to corrosion and long-term electrochemical performance of the implants. In the light of tissue damage due to corrosion, TiN appears to be a very suitable material for implants. There seems to occur no dissolution of the material [55], like with Pt [46] and IrOx [43]. As long as very high anodic potentials are avoided [34], we show that no corrosion occurs even after almost 9 million pulses. When corrosion does occur, its product (a passivation layer) remains attached to the electrodes and is not harmful to the tissue [33,55].

## 5. Conclusions

It was long suspected that in vitro safe limits established for implantable electrodes may not be applicable in vivo, which we confirm here. We also show that the type of tissue in which the electrode is implanted has an influence on safety limits. Biocompatibility and corrosion resistance cannot be viewed as two separate properties of implantable stimulation (and sensing) electrodes. Tissue responses influence the electrochemical behaviour of implanted electrodes and use of the electrodes influences the tissue surrounding the electrodes. It is therefore of great importance that safe limits are established for each electrode depending on the tissue in which it will be implanted.

**Supplementary Materials:** The following are available online at http://www.mdpi.com/2075-4701/9/4/389/s1, Figure S1: (a) Tissue around the tip of an electrode stimulated at 20 mA-200 Hz after 1 week of implantation. The tissue was stained using haematoxylin and eosin (H&E), which is the most commonly applied stain in medical diagnostics. Some inflammatory cells can still be observed but capsule formation has begun to take place. (b) Cells around the silicone part of the electrode appear very similar to those around the electrode tip, indicating no signs of stimulation-induced tissue damage. Figure S2: (a) The tissue around electrodes in group 1 showed no signs of tissue damage upon sacrifice. (b) The tissue around electrodes in group 2 showed some redness around the electrode tip, which likely is due to tissue damage. (c) The tissue around the electrode tips of electrodes in group 3 showed obvious tissue damage but the tissue around the insulated parts was unaffected. (d) The tissue around the electrode tips of electrodes in group 4 showed even more extensive tissue damage and bleeding. Nevertheless, the tissue around the insulated parts was unaffected.

**Author Contributions:** Conceptualization, S.M. and N.R.; methodology, S.M., K.R., S.S. and N.R.; writing—original draft preparation, S.M.; writing—review and editing, S.M., K.R., S.S and N.R.; project administration, N.R.; funding acquisition, N.R.

**Funding:** This research was funded by the Danish National Advanced Technology Foundation.

**Acknowledgments:** The authors thank Neurodan A/S, a member of the Ottobock group, for supplying the electrodes used in this study.

**Conflicts of Interest:** The authors declare no conflict of interest.

## References

1. Saldach, M.; Hubmann, M.; Weikl, A.; Hardt, R. Sputter-deposited TiN electrode coatings for superior pacing and sensing performance. *Pacing Clin. Electrophysiol.* **1990**, *13*, 1891–1895. [CrossRef]
2. Lau, C.P.; Tse, H.F.; Camm, A.J.; Barold, S.S. Evolution of pacing for bradycardias: Sensors. *Eur. Heart J. Suppl.* **2007**, *9*, I11–I22. [CrossRef]
3. Norlin, A.; Pan, J.; Leygraf, C. Investigation of electrochemical behavior of stimulation/sensing materials for pacemaker electrode applications: I Pt, Ti and TiN coated electrodes. *J. Electrochem. Soc.* **2005**, *152*, J7–J15. [CrossRef]
4. Hubmann, M.; Bolz, A.; Hartz, R.; Saldach, M. Long term performance of stimulation and sensing behaviour of TiN and Ir coated pacemaker lead having a fractal surface structure. In Proceedings of the 1992 14th Annual International Conference of the IEEE Engineering in Medicine and Biology Society, Paris, France, 29 October–1 November 1992; Volume 6.
5. Janders, M.; Egert, U.; Stelzle, M.; Nisch, W. Novel thin film titanium nitride micro-electrodes with excellent charge transfer capability for cell stimulation and sensing applications. In Proceedings of the 1996 18th Annual International Conference of the IEEE Engineering in Medicine and Biology Society, Amsterdam, The Netherlands, 31 October–3 November 1 1996; Volume 1.
6. Zhou, D.M.; Greenberg, R.J. Electrochemical characterization of titanium nitride microelectrode arrays for charge-injection applications. In Proceedings of the 2003 25th Annual International Conference of the IEEE Engineering in Medicine and Biology Society, Cancun, Mexico, 17–21 September 2003; Volume 2.
7. Kane, S.R.; Cogan, S.F.; Ehrlich, J.; Plante, T.D.; McCreery, D.B.; Troyk, P.R. Electrical performance of penetrating microelectrodes chronically implanted in cat cortex. *IEEE Trans. Biomed. Eng.* **2013**, *60*, 2153–2160. [CrossRef] [PubMed]
8. Brunton, E.K.; Winther-Jensen, B.; Wang, C.; Yan, E.B.; Hagh Gooie, S.; Lowery, A.J.; Rajan, R. In vivo comparison of the charge densities required to evoke motor responses using novel annular penetrating microelectrodes. *Front. Neurosci.* **2015**, *9*, 265. [CrossRef]

9. Weiland, J.D.; Anderson, D.J.; Humayun, M.S. In vitro electrical properties for iridium oxide versus titanium nitride stimulating electrodes. *IEEE Trans. Biomed. Eng.* **2002**, *49*, 1574–1579. [CrossRef]
10. Cogan, S.F. Neural stimulation and recording electrodes. *Annu. Rev. Biomed. Eng.* **2008**, *10*, 275–309. [CrossRef] [PubMed]
11. Cogan, S.F.; Troyk, P.R.; Ehrlich, J.; Plante, T.D. In vitro comparison of the charge-injection limits of activated iridium oxide (AIROF) and platinum-iridium microelectrodes. *IEEE Trans. Biomed. Eng.* **2005**, *52*, 1612–1614. [CrossRef] [PubMed]
12. Cogan, S.F.; Troyk, P.R.; Ehrlich, J.; Plante, T.D.; Detlefsen, D.E. Potential-biased, asymmetric waveforms for charge-injection with activated iridium oxide (AIROF) neural stimulation electrodes. *IEEE Trans. Biomed. Eng.* **2006**, *53*, 327–332. [CrossRef] [PubMed]
13. Whalen, J.J.; Young, J.; Weiland, J.D.; Searson, P.C. Electrochemical characterization of charge injection at electrodeposited platinum electrodes in phosphate buffered saline. *J. Electrochem. Soc.* **2006**, *153*, C834–C839. [CrossRef]
14. Cogan, S.F.; Troyk, P.R.; Ehrlich, J.; Gasbarro, C.M.; Plante, T.D. The influence of electrolyte composition on the in vitro charge-injection limits of activated iridium oxide (AIROF) stimulation electrodes. *J. Neural Eng.* **2007**, *4*, 79–86. [CrossRef] [PubMed]
15. Cogan, S.F.; Ehrlich, J.; Plante, T.D.; Smirnov, A.; Shire, D.B.; Gingerich, M.; Rizzo, J.F. Sputtered iridium oxide films for neural stimulation electrodes. *J. Biomed. Mater. Res. B* **2009**, *89*, 353–361. [CrossRef]
16. Cogan, S.F.; Ehrlich, J.; Plante, T.D. The effect of electrode geometry on electrochemical properties measured in saline. In Proceedings of the 2014 36th Annual International Conference of the IEEE Engineering in Medicine and Biology Society (EMBC), Chicago, IL, USA, 26–30 August 2014.
17. Boehler, C.; Stieglitz, T.; Asplund, M. Nanostructured platinum grass enables superior impedance reduction for neural microelectrodes. *Biomaterials* **2015**, *67*, 346–353. [CrossRef] [PubMed]
18. Weremfo, A.; Carter, P.; Hibbert, D.B.; Zhao, C. Investigating the interfacial properties of electrochemically roughened platinum electrodes for neural stimulation. *Langmuir* **2015**, *31*, 2593–2599. [CrossRef]
19. Ghazavi, A.; Cogan, S.F. Electrochemical characterization of high frequency stimulation electrodes: Role of electrode material and stimulation parameters on electrode polarization. *J. Neural Eng.* **2018**, *15*, 036023. [CrossRef]
20. Deku, F.; Joshi-Imre, A.; Mertiri, A.; Gardner, T.J.; Cogan, S.F. Electrodeposited Iridium Oxide on Carbon Fiber Ultramicroelectrodes for Neural Recording and Stimulation. *J. Electrochem. Soc.* **2018**, *165*, D375–D380. [CrossRef]
21. Wei, X.F.; Grill, W.M. Impedance characteristics of deep brain stimulation electrodes in vitro and in vivo. *J. Neural Eng.* **2009**, *6*, 046008. [CrossRef] [PubMed]
22. Leung, R.T.; Shivdasani, M.N.; Nayagam, D.A.; Shepherd, R.K. In vivo and in vitro comparison of the charge injection capacity of platinum macroelectrodes. *IEEE Trans. Biomed. Eng.* **2015**, *62*, 849–857. [CrossRef]
23. Meijs, S.; Fjorback, M.; Jensen, C.; Sørensen, S.; Rechendorff, K.; Rijkhoff, N.J.M. Electrochemical properties of titanium nitride nerve stimulation electrodes: An in vitro and in vivo study. *Front. Neurosci.* **2015**, *9*, 268. [CrossRef] [PubMed]
24. Meijs, S.; Fjorback, M.; Jensen, C.; Sørensen, S.; Rechendorff, K.; Rijkhoff, N.J.M. Influence of fibrous encapsulation on electro-chemical properties of TiN electrodes. *Med. Eng. Phys.* **2016**, *38*, 468–476. [CrossRef] [PubMed]
25. Meijs, S.; Sørensen, C.; Sørensen, S.; Rechendorff, K.; Fjorback, M.; Rijkhoff, N.J.M. Influence of implantation on the electrochemical properties of smooth and porous TiN coatings for stimulation electrodes. *J. Neural Eng.* **2016**, *13*, 026011. [CrossRef] [PubMed]
26. Meijs, S.; Alcaide, M.; Sørensen, C.; McDonald, M.; Sørensen, S.; Rechendorff, K.; Gerhardt, A.; Nesladek, M.; Rijkhoff, N.J.; Pennisi, C.P. Biofouling resistance of boron-doped diamond neural stimulation electrodes is superior to titanium nitride electrodes in vivo. *J. Neural Eng.* **2016**, *13*, 056011. [CrossRef] [PubMed]
27. Black, B.J.; Kanneganti, A.; Joshi-Imre, A.; Rihani, R.; Chakraborty, B.; Abbott, J.; Pancrazio, J.J.; Cogan, S.F. Chronic recording and electrochemical performance of Utah microelectrode arrays implanted in rat motor cortex. *J. Neurophys.* **2018**, *120*, 2083–2090. [CrossRef] [PubMed]
28. Lempka, S.F.; Miocinovic, S.; Johnson, M.D.; Vitek, J.L.; McIntyre, C.C. In vivo impedance spectroscopy of deep brain stimulation electrodes. *J. Neural Eng.* **2009**, *6*, 046001. [CrossRef] [PubMed]

29. Cyster, L.A.; Grant, D.M.; Parker, K.G.; Parker, T.L. The effect of surface chemistry and structure of titanium nitride (TiN) films on primary hippocampal cells. *Biomol. Eng.* **2002**, *19*, 171–175. [CrossRef]
30. Cyster, L.A.; Parker, K.G.; Parker, T.L.; Grant, D.M. The effect of surface chemistry and nanotopography of titanium nitride (TiN) films on 3T3-L1 fibroblasts. *J. Biomed. Mater. Res. A* **2003**, *67*, 138–147. [CrossRef]
31. Cyster, L.A.; Parker, K.G.; Parker, T.L.; Grant, D.M. The effect of surface chemistry and nanotopography of titanium nitride (TiN) films on primary hippocampal neurones. *Biomaterials* **2004**, *25*, 97–107. [CrossRef]
32. Massiani, Y.; Medjahed, A.; Crousier, J.P.; Gravier, P.; Rebatel, I. Corrosion of sputtered titanium nitride films deposited on iron and stainless steel. In *Metallurgical Coatings and Materials Surface Modifications*; Hintermann, H.E., Spitz, J., Eds.; North-Holland: Amsterdam, The Netherlands, 1991; pp. 115–120.
33. Avasarala, B.; Haldar, P. Electrochemical oxidation behavior of titanium nitride based electrocatalysts under PEM fuel cell conditions. *Electrochim. Acta* **2010**, *55*, 9024–9034. [CrossRef]
34. Norlin, A.; Pan, J.; Leygraf, C. Investigation of Pt, Ti, TiN and nano-porous carbon electrodes for implantable cardioverter-defibrillator applications. *Electrochim. Acta* **2004**, *49*, 4011–4020. [CrossRef]
35. Merrill, D.R.; Bikson, M.; Jefferys, J.G. Electrical stimulation of excitable tissue: Design of efficacious and safe protocols. *J. Neurosci. Methods* **2005**, *141*, 171–198. [CrossRef]
36. Ragheb, T.; Geddes, L.A. Electrical properties of metallic electrodes. *Med. Biol. Eng. Comput.* **1990**, *28*, 182–186. [CrossRef]
37. Meng, L.J.; Santos, M.D. Characterization of titanium nitride films prepared by dc reactive magnetron sputtering at different nitrogen pressures. *Surf. Coat. Technol.* **1997**, *90*, 64–70. [CrossRef]
38. Chawla, V.; Jayaganthan, R.; Chandra, R. Structural characterizations of magnetron sputtered nanocrystalline TiN thin films. *Mater. Charact.* **2008**, *59*, 1015–1020. [CrossRef]
39. Cunha, L.T.; Pedrosa, P.; Tavares, C.J.; Alves, E.; Vaz, F.; Fonseca, C. The role of composition, morphology and crystalline structure in the electrochemical behaviour of TiNx thin films for dry electrode sensor materials. *Electrochim. Acta* **2009**, *55*, 59–67. [CrossRef]
40. Sánchez, G.; Rodrigo, A.; Bologna Alles, A. Titanium nitride pacing electrodes with high surface-to-area ratios. *Acta Mater.* **2005**, *53*, 4079. [CrossRef]
41. Brummer, S.B.; Turner, M.J. Electrical stimulation with Pt electrodes: II-estimation of maximum surface redox (theoretical non-gassing) limits. *IEEE Trans. Biomed. Eng.* **1977**, *5*, 440–443. [CrossRef]
42. McHardy, J.; Robblee, L.S.; Marston, J.M.; Brummer, S.B. Electrical stimulation with Pt electrodes. IV. Factors influencing Pt dissolution in inorganic saline. *Biomaterials* **1980**, *1*, 129–134. [CrossRef]
43. Negi, S.; Bhandari, R.; Rieth, L.; Van Wagenen, R.; Solzbacher, F. Neural electrode degradation from continuous electrical stimulation: Comparison of sputtered and activated iridium oxide. *J. Neurosci. Methods* **2010**, *186*, 8–17. [CrossRef]
44. Musa, S.; Rand, D.R.; Bartic, C.; Eberle, W.; Nuttin, B.; Borghs, G. Coulometric detection of irreversible electrochemical reactions occurring at Pt microelectrodes used for neural stimulation. *Anal. Chem.* **2011**, *83*, 4012–4022. [CrossRef]
45. Norlin, A.; Pan, J.; Leygraf, C. Investigation of interfacial capacitance of Pt, Ti and TiN coated electrodes by electrochemical impedance spectroscopy. *Biomol. Eng.* **2002**, *19*, 67–71. [CrossRef]
46. Robblee, L.S.; McHardy, J.; Marston, J.M.; Brummer, S.B. Electrical stimulation with Pt electrodes. V. The effect of protein on Pt dissolution. *Biomaterials* **1980**, *1*, 135–139. [CrossRef]
47. Robblee, L.S.; McHardy, J.; Agnew, W.F.; Bullara, L.A. Electrical stimulation with Pt electrodes. VII. Dissolution of Pt electrodes during electrical stimulation of the cat cerebral cortex. *J. Neurosci. Methods* **1983**, *9*, 301–308. [CrossRef]
48. Shepherd, R.K.; Murray, M.T.; Hougiton, M.E.; Clark, G.M. Scanning electron microscopy of chronically stimulated platinum intracochlear electrodes. *Biomaterials* **1985**, *6*, 237–242. [CrossRef]
49. Hibbert, D.B.; Weitzner, K.; Tabor, B.; Carter, P. Mass changes and dissolution of platinum during electrical stimulation in artificial perilymph solution. *Biomaterials* **2000**, *21*, 2177–2182. [CrossRef]
50. McCreery, D.B.; Agnew, W.F.; Yuen, T.G.H.; Bullara, L.A. Relationship between stimulus amplitude, stimulus frequency and neural damage during electrical stimulation of sciatic nerve of cat. *Med. Biol. Eng. Comput.* **1995**, *33*, 426–429. [CrossRef]
51. Cogan, S.F.; Ludwig, K.A.; Welle, C.G.; Takmakov, P. Tissue damage thresholds during therapeutic electrical stimulation. *J. Neural Eng.* **2016**, *13*, 021001. [CrossRef] [PubMed]

52. Meijs, S. The Influence of Tissue Responses on the Electrochemical Properties of Implanted Neural Stimulation Electrodes. Ph.D. Thesis, Aalborg Universitetsforlag, Aalborg, Denmark, 20 May 2016.
53. Loeb, G.E.; Richmond, F.J.; Baker, L.L. The BION devices: Injectable interfaces with peripheral nerves and muscles. *Neurosurg. Focus* **2006**, *20*, 1–9. [CrossRef]
54. Majid, A. *Electroceuticals*, 1st ed.; Springer: Basel, Switzerland, 2017.
55. Datta, S.; Das, M.; Balla, V.K.; Bodhak, S.; Murugesan, V.K. Mechanical, wear, corrosion and biological properties of arc deposited titanium nitride coatings. *Surf. Coat. Technol.* **2018**, *344*, 214–222. [CrossRef]